Simulating Raman Scattering Impairments with Depolarization Noise in Quantum-Classical Links

Simulating Raman Scattering Impairments with Depolarization Noise in Quantum-Classical Links

Jake Smith, Roberto Proietti
Polytechnic University of Turin. Corso Duca degli Abruzzi, 24, 10129 Turin TO, Italy.
jake.smith@polito.it, roberto.proietti@polito.it

Abstract: *We model spontaneous Raman scattering noise in polarization-encoded quantum communication channels co-propagating with classical signals using the depolarization channel. Utilizing NetSquid simulations, we validate the model against demonstrations of qubit transmission, entanglement distribution, and teleportation.*
Keywords: Photonic quantum communication, Photonic quantum information processing.

I. Introduction

In recent years, quantum networks have made significant progress in using photonic qubits to interconnect quantum processors, either through direct qubit transmission or by leveraging nonlocal correlations to teleport quantum states and mitigate optical fiber loss. Quantum networks are dependent on classical control planes to share outcomes of network primitives, such as Bell-state measurements (BSM), making quantum-classical fibre coexistence desirable for practical implementations. To reduce deployment cost, quantum signals should be integrated within existing infrastructure rather than building stand-alone quantum networks. Coexisting entanglement distribution has been demonstrated using wavelength-division multiplexing with suitable visibility to violate the Bell-inequality [1, 2, 3].

Coexistence demonstrations have raised questions about modeling classical noise, particularly nonlinear spontaneous Raman scattering (SpRS), in quantum networks. SpRS noise is typically quantified by the detected Raman power based on various fibre and detector parameters, however, this framework is not suitable for use in many quantum network simulators. Such simulators [4] model a subset of the network stack, such as analytical point-to-point simulators [5] or event-based simulators of network protocols [6, 7]. The latter abstract hardware and qubit encoding to model noise with theoretical quantum channels, preventing the incorporation of hardware parameters into the simulator's error modeling. Consequently, these simulators are currently unable to estimate the coexisting SpRS noise effects on abstract qubits and quantum network primitives [8].

In this work, we address this gap by proposing a framework to translate coexisting SpRS noise into a format compatible with quantum network simulators. Previous work [1, 2, 3] identifies SpRS photons generated at the quantum wavelength by the higher power classical channel as the dominant noise source for coexisting quantum channels. Experiments characterize SpRS noise photons generated from a C-band source as completely depolarized with a purity $P = 0.5$, and their detection noise on the polarization-encoded qubit ρ is well described by the depolarization channel $\varepsilon_{Dep}(\rho)$ with mixing probability p_m [1].

$$\varepsilon_{Dep}(\rho) = \left(1 - \frac{3p_m}{4}\right)\rho + \frac{p_m}{4}\left(\sigma_x\rho\sigma_x + \sigma_y\rho\sigma_y + \sigma_z\rho\sigma_z\right) \tag{1}$$

We analytically derive the depolarization channel's mixing probability p_m from physical parameters and validate the model using NetSquid [6] versus recent implementations of direct transmission [1], entanglement distribution [2], and teleportation [3] of polarization-encoded qubits coexisting with a classical channel.

II. Derivation of Depolarization Channel Mixing Probability

A. Direct Qubit Transmission Noise Model

When transmitting polarization-encoded qubits across a coexisting channel, the probability of mixing p_m is related to the incident Raman photons detected at the quantum wavelength. The average number of detected SpRS photons n_{SpRS} within a detection window ΔT is defined as [9]

$$n_{SpRS} = \beta(\lambda_q, \lambda_c) L_{eff} \frac{P_L}{E_{ph}(\lambda_q)} \Delta\lambda \Delta T \eta_d = R_{SpRS} \Delta\lambda \Delta T \eta_d \tag{2}$$

where β is the SpRS coefficient quantifying the amount of the Raman gain effect at the quantum wavelength λ_q, P_L is the launch power into the fibre, $\Delta\lambda$ is the quantum filter bandwidth, η_d is the efficiency of detector, and R_{SpRS} is the rate of incident SpRS photons. L_{eff} is the effective length of the fibre with co- or counter-propagating Raman scattering [6]. Normalizing this amount by the average number of detection events yields the mixing probability

This work was supported by SVCF 2023-328132.

$$p_m = \frac{n_{SpRS}}{n_{SpRS} + n_q} \tag{3}$$

where n_q is the average number of qubits detected per ΔT [1].

B. *Entanglement Distribution Noise Model*

Distributing polarization-encoded Bell states from a spontaneous parametric down-conversion (SPDC) source requires adapting the direct transmission noise model to incorporate the hardware noise of the source and the paired superconducting nanowire single-photon detectors. Building on the approach in [3, 10], the visibility of the entangled source V_{ent} must be estimated from the probability of detecting a Raman photon p_{SpRS} within each detection window. With effective spectro-temporal filtering, p_{SpRS} can be assumed to be << 1. With this assumption, the probability of detection at the end of fibre i is

$$p_{SpRS_i} = n_{SpRS_i}\eta_{d_i}\eta_{rx_i} + \eta_i\mu_{N_i} + d_i \tag{4}$$

where η_{rx_i} is the transmission efficiency of the receiver's optical components, η_i is the total transmission efficiency from emitter to detection at the receiver, μ_{N_i} represents the average number of noise photons generated per pulse at the quantum source, and d_i is the dark counts per detection window. n_{SpRS_i} can be treated as a cumulative detection noise term if other sources of noise are characterized. For η_i << 1, μ_s << 1, and p_{SpRS_i} << 1, the maximum and minimum coincidence counts, $C_{(i,j)}$ and $A_{(i,j)}$, including noisy detections are approximated from the single count probability S_i

$$S_i \approx \eta_i\mu_s + p_{SpRS_i},\ C_{(i,j)} \approx \eta_i\eta_j(\mu_s + \mu_s^2) + S_iS_j,\ A_{(i,j)} \approx S_iS_j \tag{5, 6, 7}$$

where μ_s is the mean photons generated per pulse [3]. Correspondingly,

$$V_{ent_{(i,j)}} = \frac{C_{(i,j)} - A_{(i,j)}}{C_{(i,j)} + A_{(i,j)}},\ F_{ent_{(i,j)}} = \frac{1 + 3V_{ent_{(i,j)}}}{4} \tag{8, 9}$$

When only one qubit experiences depolarization noise, $p_{m_{(i,j)}} = 1 - F_{ent_{(i,j)}}$ [11]. The p_m of different entanglement distribution topologies can be compared using n_{SpRS} [5]. A source-at-sender which only co-propagates the signal can set $n_{SpRS_{idler}} = 0$. A midpoint source can instead set $L_{eff_{signal}} = L_{eff_{idler}}$.

III. Simulating Coexisting SpRS Noise in NetSquid

We utilize NetSquid to validate the depolarization model's output versus coexistence demonstrations. All studies employ a C-band source to co-propagate with either C-band [1] or O-band polarization-encoded qubits [2, 3]. Each study reports the baseline fidelity of the transmitted state in the absence of the classical channel ρ_{dark} with its pure state ψ such that $F_{dark} = F(\psi, \rho_{dark})$. In NetSquid, ρ_{dark} is represented using the density operator. The sender node prepares ρ_{dark} with experimentally characterized F_{dark} before transmitting across a coexisting fiber to the receiving node. Within the simulated fibre, coexisting SpRS detection noise is applied using the depolarization channel with the derived p_m to output the noisy coexisting state ρ_{coex} at the receiver.

Chapman et al. approximate a single photon source using attenuated coherent states across 1530-1570 nm quantum channels co-propagating with a 1542.5 nm classical source at ~5.5 dBm over various fiber lengths [1]. In NetSquid, we emulate the 5.5 km configuration, where ρ_{dark} is estimated using the Bloch sphere parameterization for the density matrix [12]. The p_m for each channel configuration is calculated from Eq. 3 using experimental n_{SpRS} and n_q counts. The dark and coexisting fidelities of each wavelength are reported with respect to the reference channel at ~1530 nm.

Thomas et al. generate polarization-entangled photons at signal and idler frequencies of 1287 and 1313 nm [2]. The signal is multiplexed with a 1550nm classical pump using a range of launch powers, while the idler propagates in dark fiber. In NetSquid, the polarization noise of ρ_{dark} is assumed to be uncompensated polarization mode dispersion or polarization-dependent loss, therefore the density matrix of ρ_{dark} is estimated by applying the dephasing channel to the pure Bell-state as shown in [13]. The p_m is derived for each P_{launch} from Eq. 8 using experimental coexisting visibility data.

Thomas et al. also perform teleportation with a midpoint BSM between Alice's polarization-encoded qubit ψ_A at 1290 nm and Bob's entangled photons at 1290 and 1310 nm [3]. ψ_A is multiplexed with a 1547.32 nm classical signal at 74 mW and propagates 15.2 km until reaching the BSM components. The classical signal is demultiplexed before the BSM and remultiplexed with Bob's signal photon where it experiences counter-propagating noise over 15 km. In NetSquid, Bob's ρ_{dark} is represented in the same manner as the entanglement scenario [13]. The dark fidelity of each state is estimated from Eq. 4 using experimental parameters and setting $n_{SpRS_i} = 0$. The respective p_m for each quantum state are derived from Eq. 4 and experimental n_{SpRS_i} counts for each signal and idler channel pair. After transmission, we first use noiseless quantum gates to perform the BSM operation on Alice's depolarized qubit σ_A and Bob's depolarized signal photon, followed by local corrections to Bob's idler.

IV. RESULTS

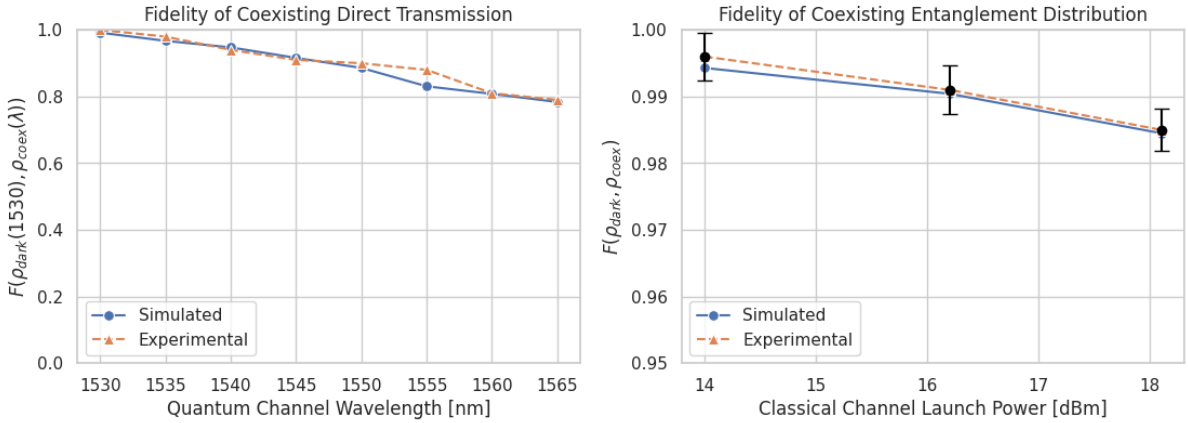

Fig. 1. Experimental and simulated quantum state fidelities of coexisting (a) direct transmission versus quantum channel wavelength, and (b) entanglement distribution versus launch power.

The simulations accurately estimate the SpRS noise imparted on qubits in each scenario. Fig. 1(a) compares the coexisting fidelity of direct qubit transmission at various wavelengths with Chapman's experimental results [1], such that $F_{coex}(\lambda) = F\big(\rho_{dark}(1530), \rho_{coex}(\lambda)\big)$. Raman gain is experimentally characterized as minimal near the classical channel and peaks near 1533 and 1555 nm [1]. At wavelengths below the classical channel, fidelity is primarily affected by SpRS noise, while higher wavelengths also suffer from greater source impurity. We find that the simulated fidelity aligns well with the experimental trend, though it slightly underestimates near 1555 nm. This discrepancy may be caused by a mischaracterized experimental source fidelity or n_{SpRS} at this wavelength.

In Fig. 1(b), we compare the simulated fidelity of coexisting entanglement distribution to Thomas's results [2], where $F_{coex} = F(\rho_{dark}, \rho_{coex})$. The simulations follow the experimental trend of decreasing fidelity with greater launch power due to more incident Raman photons at the detector. The fidelity of this experiment is significantly higher than the previous due to improved wavelength selection and spectro-temporal filtering techniques. Thomas [2] chooses to co-propagate qubits in the O-band resulting in lower Raman gain at these wavelengths from the C-band source than Chapman's C-band quantum and classical channels [1].

In Table I, we report high accuracy between experimental and simulated teleportation fidelity values of pole, equatorial, and average states on the Bloch sphere. As performed in [3], the coexisting fidelity calculation is dependent on the location of ψ_A on the Bloch sphere. Pole state fidelity is dependent on $F_{Alice} = F(\psi_A, \sigma_A)$ and the entanglement fidelity, which are calculated from NetSquid simulations. Calculating equatorial state fidelity additionally requires estimating Hong-Ou-Mandle (HOM) interference visibility, V_{HOM}. Deriving the effect of SpRS on V_{HOM} is beyond this paper's scope and covered in [10]. The average fidelity of an arbitrary qubit is derivable from both the pole and equatorial fidelities. In addition to simulated F_{Alice} and entanglement fidelity, we utilize Thomas's experimental dark V_{HOM} = 83.1 +/- 1.4 and coexisting V_{HOM} = 80.3 +/- 3.8% to compute $F_{equatorial}$ and $F_{average}$ [3].

TABLE I: FIDELITY OF COEXISTING TELEPORTATION

	Dark Fibre [3]	Simulated Dark Fibre	Coex. Fibre [3]	Simulated Coex. Fibre
F_{poles}	97.6	97.5	96.7	96.5
$F_{equatorial}$	90.2	90.0 +/- 2.1	88.7 +/- 3.8	87.4 +/- 1.8
$F_{average}$	92.7	92.5 +/- 1.4	89.9 +/- 3.1	90.4 +/- 1.2

V. CONCLUSIONS

We present the first theoretical model to translate coexisting SpRS noise into the depolarization channel for use within quantum network simulators. The model demonstrates high accuracy in reproducing experimental fidelity across coexisting direct transmission, entanglement distribution, and teleportation demonstrations. The results highlight the ability of quantum channel theory to model coexisting polarization noise affecting arbitrary quantum states. This framework will enable simulators to optimize coexisting network operations at the Physical layer and above. Channel configurations can be evaluated to maximize the estimated fidelity of quantum network primitives. Competing entanglement distribution and network topologies invoking noisy primitives can be compared for different use-cases, such as theorized quantum data-centers [5, 14]. This model will aid the ongoing evaluation of photonic hardware to meet the performance requirements of quantum communication and distributed computing in coexisting networks.

ACKNOWLEDGMENT

We would like to thank Dr. Carrie Weidner for her engaging discussions about state representations.

REFERENCES

[1] Chapman, J. C., Lukens, J. M., Alshowkan, M., Rao, N., Kirby, B. T., & Peters, N. A. (2023). Coexistent quantum channel characterization using spectrally resolved Bayesian quantum process tomography. *Physical Review Applied*, *19*(4), 044026.

[2] Thomas, J. M., Kanter, G. S., & Kumar, P. (2023). Designing noise-robust quantum networks coexisting in the classical fiber infrastructure. *Optics Express*, *31*(26), 43035-43047.

[3] Thomas, J. M., Yeh, F. I., Chen, J. H., Mambretti, J. J., Kohlert, S. J., Kanter, G. S., & Kumar, P. (2024). Quantum teleportation coexisting with classical communications in optical fiber. *Optica*, *11*(12), 1700-1707.

[4] Bel, O., & Kiran, M. (2024). Simulators for quantum network modelling: A comprehensive review. *arXiv preprint arXiv:2408.11993*.

[5] Beukers, H. K., Pasini, M., Choi, H., Englund, D., Hanson, R., & Borregaard, J. (2023). Tutorial: Remote entanglement protocols for stationary qubits with photonic interfaces. *arXiv preprint arXiv:2310.19878*.

[6] Coopmans, T., Knegjens, R., Dahlberg, A., Maier, D., Nijsten, L., de Oliveira Filho, J., ... & Wehner, S. (2021). NetSquid, a network simulator for quantum information using discrete events. *Communications Physics*, *4*(1), 164.

[7] Satoh, R., Hajdušek, M., Benchasattabuse, N., Nagayama, S., Teramoto, K., Matsuo, T., ... & Van Meter, R. (2022, September). Quisp: a quantum internet simulation package. In *2022 IEEE International Conference on Quantum Computing and Engineering (QCE)* (pp. 353-364). IEEE.

[8] Yan, X., Gitt, S., Lin, B., Witt, D., Abdolahi, M., Afifi, A., ... & Young, J. F. (2021). Silicon photonic quantum computing with spin qubits. *APL Photonics*, *6*(7).

[9] Fröhlich, B., Dynes, J. F., Lucamarini, M., Sharpe, A. W., Tam, S. W. B., Yuan, Z., & Shields, A. J. (2015). Quantum secured gigabit optical access networks. *Scientific reports*, *5*(1), 18121.

[10] Thomas, Jordan; Yeh, Fei; Chen, Jim; Mambretti, Joe; Kohlert, Scott; Kanter, Gregory; et al. (2024). Supplementary document for Quantum Teleportation Coexisting with Classical Communications in Optical Fiber - 7260233.pdf. Optica Publishing Group. Journal contribution. https://doi.org/10.6084/m9.figshare.27316089.v2

[11] Preskill, J. (1998). Lecture notes for physics 229: Quantum information and computation. *California institute of technology*, *16*(1).

[12] Klimov, A. B., & Sánchez-Soto, L. L. (2010). Depolarization for quantum channels with higher symmetries. *Physica Scripta*, *2010*(T140), 014009.

[13] Liu, Y. (2023). Decoherence-free subspace and entanglement sudden death of multi-photon polarization states in fiber channels. *Communications in Theoretical Physics*, *75*(4), 045104.

[14] Shapourian, H., Kaur, E., Sewell, T., Zhao, J., Kilzer, M., Kompella, R., & Nejabati, R. (2025). Quantum Data Center Infrastructures: A Scalable Architectural Design Perspective. *arXiv preprint arXiv:2501.05598*.